

Cepheids in NGC 1866 - a Test for Pulsational Models

Giuseppe Bono¹ & Marcella Marconi²

¹Trieste Astronomical Observatory, Via G. B. Tiepolo 11, 34131 Trieste, Italy - E-Mail: bono@oat.ts.astro.it

²Dept. of Physics, University of Pisa, Piazza Torricelli 2, 56100 Pisa, Italy - E-Mail: marcella@astr1pi.difi.unipi.it

ABSTRACT

We present nonlinear theoretical results concerning the predicted pulsational behaviour of stellar models suitable for the sample of Cepheids belonging to the Large Magellanic Cloud (LMC) star cluster NGC 1866. The blue and red edges of the instability strip, transformed into the observative plane (V, B-V) by adopting current values for the distance modulus (DM=18.57 mag., Welch et al. 1991) and for the reddening (E(B-V)=0.06 mag., Arp 1967; Walker 1974; Walker 1987), are in agreement with the observed distribution of Cepheids in the quoted cluster. Moreover, the distribution of observational data in the Bailey diagram (V amplitude versus period) appears in agreement with theoretical predictions derived adopting the luminosity level predicted by canonical evolutionary models. The role played by the direct *ab initio* integration of the coupling between pulsation and convection and by the input physics on the smoothness of light and velocity curves is briefly discussed.

Key words: Cepheids – Magellanic Clouds – Globular Clusters: individual (NGC 1866) – stars: oscillations

1 INTRODUCTION

The LMC globular cluster NGC 1866 has been already used extensively for testing stellar evolutionary models and for shedding light on some problems currently debated in the literature (Chiosi et al. 1989; Brocato, Castellani & Pier-simoni 1994). This cluster is also expected to play a key role in the theory of stellar pulsation, since it provides a beautiful sample of 23 Cepheids with a common value for both distance modulus and reddening. Welch et al. (1991, hereinafter referred to as WCFMM) already disclosed that this sample of radial pulsators shows a well defined instability strip which is not revealed by current data on Galactic Cepheids, and represents a fundamental benchmark for both modal stabilities (fundamental and first overtone) and pulsational amplitudes predicted by theoretical models.

As a first step of an extended and detailed investigation of Cepheid hydrodynamical models we use NGC 1866 to test both the accuracy and the internal consistency of the theoretical framework we developed for evaluating the approach to limit cycle stability and the predicted pulsational amplitudes. The main aim of this paper is to discuss the comparison between a new set of limiting amplitude, nonlinear, nonlocal and time-dependent convective models and the observational constraints provided by this cluster. In §2 the theoretical results are briefly discussed while §3 presents the comparison with the sample of Cepheids in NGC 1866 for which magnitudes, colours, and pulsational amplitudes are currently available. The last section summarizes the main results of this investigation and outlines future theoretical and observational perspectives.

2 THEORETICAL FRAMEWORK

According to current evolutionary predictions for Cepheids in NGC 1866, we adopted a fixed stellar mass ($M/M_{\odot}=5.0$). Even though no direct estimation of the metallicity of this cluster has been provided yet, we adopted the metal abundance obtained by Russell & Bessell (1989) and Russel & Dopita (1990) for young LMC stars, i.e. $Z=0.008$. We also adopted the helium content $Y=0.25$ provided by Dufour (1984) on the basis of He abundance evaluations in H II regions. Similar physical parameters have also been assumed by Chiosi et al. (1992,1993 and references therein) in their extensive investigation of the pulsational properties of Cepheids linear models. For properly evaluating the topology of the instability strip we computed four sequences of both linear and nonlinear models located at different luminosity levels ($\log L/L_{\odot} = 2.80, 3.07, 3.3, 3.6$) which cover a wide effective temperature range ($4800 \leq T_e \leq 6700$ K). The location of the blue and red edges of fundamental and first overtone pulsators has been evaluated by adopting, close to these boundaries, a temperature step of 100 K. The theoretical framework adopted for evaluating the pulsational properties of Cepheids has already been described in a series of previous papers (Bono & Stellingwerf 1993,1994; Bono et al. 1997b and references therein). In this section we only discuss the main differences with the quoted investigations concerning the physical assumptions adopted to approach Cepheids pulsational models.

For providing a good spatial resolution throughout the envelope model, the static structures have been computed by

adopting an outer boundary optical depth $\tau = 0.0001$. At the same time, the mass ratio (h) between consecutive zones has been assumed equal to 1.04 in the stellar layers located at temperatures lower than 6.0×10^4 K, whereas for higher temperatures we adopted $h=1.2$. The inner boundary has been fixed so that the base of the envelope was approximately located at a distance from the stellar centre of the order of 10% of the photospheric radius (i.e. $r_0 = 0.1 \times R_{ph}$). Unlike envelope models of low-mass stars, these assumptions ensure that the mass included in a typical Cepheid model ranges from 40 to 50 percent of the total stellar mass. Both linear and nonlinear models have been computed by adopting the radiative opacity tables recently provided by Iglesias & Rogers (1996) for temperatures higher than 10,000 K, and the molecular opacities provided by Alexander & Ferguson (1994) for lower temperatures. The method adopted for handling the opacity tables is described in Bono, Incerpi & Marconi (1996).

The nonlinear analysis has been performed by perturbing the linear radial eigenfunction of the first two modes with a constant velocity amplitude of 10 km/sec. In contrast with nonlinear RR Lyrae and Type II Cepheid models, which have been computed with timesteps fixed by the CFL condition for properly handling the development and propagation of the shock front along the pulsation cycle, the nonlinear Cepheid models have been computed by adopting a number of timesteps per period which range from 300 for first overtone models to 400 for fundamental pulsators. This choice is due to the evidence that along a full cycle Cepheid models develop only mild shocks in the hydrogen and helium ionization regions. As a test, few selected models computed by adopting the CFL conditions do not present any substantial difference in the pulsation amplitudes in comparison with the models computed by adopting a fixed timestep. The number of pulsation cycles needed to approach the asymptotic amplitudes depends on the location of the model inside the instability strip and ranges from 1,000 to more than 10,000.

A thorough comparison of our models with both linear (Chiosi et al. 1993; Morgan & Welch 1996) and nonlinear radiative Cepheid models (Sebo & Wood 1995; Simon & Kanbur 1995; Buchler et al. 1996), together with a detailed analysis of the physical structure of the envelope models will be discussed in a forthcoming paper (Bono & Marconi 1997). The top panel of Figure 1 shows a selected sample of fundamental and first overtone bolometric light curves located at $\log L/L_\odot = 3.07$, i.e. at the luminosity level predicted by canonical evolutionary models. The first interesting result is that moving from the blue to the red edge of the instability strip the light curves show smooth changes along the pulsation cycle and do not present, at least in this period range, any peculiar bump and/or dip. The comparison with results available in the literature (Karp 1975; Carson & Stothers 1984) strengthens the key role played by the inclusion of a time-dependent treatment of convective transport which reduces the pulsational amplitudes and at the same time ensures a smooth excursion of physical variables across the ionization regions. The bottom panel of Figure 1 shows the surface radial velocities of the same models shown in the top panel. The smoothness of these curves over the pulsation

Figure 1. *Top:* Selected bolometric light curves as a function of the pulsational phase. Solid and dashed lines are referred to first overtone and fundamental pulsators respectively. The magnitude scale is referred to the top curve; the other ones have been artificially shifted by -0.60 mag. The nonlinear periods are also labelled. *Bottom:* Surface radial velocity curves of the models plotted in the top panel. The velocity scale is referred to the top curve; the other ones have been artificially shifted by -35 km/sec. The effective temperatures are also labelled.

cycle is the result of a long *ab initio* integration time during which the radial motions approach their asymptotic amplitudes and the spurious high-order modes introduced by the initial perturbation settle down. A more detailed summary of the nonlinear observables obtained in the present investigation for both fundamental and first overtone pulsators is given in Table 1. This table presents from left to right the logarithmic luminosity, the effective temperature, the nonlinear pulsation period, and the fractional radius variation, i.e. $\Delta R/R_{ph} = (R^{max} - R^{min})/R_{ph}$, where R_{ph} is the photospheric radius. Column (5) reports the "pure" radial velocity amplitude of the surface zone, i.e. no correction factor for limb darkening has been taken into account. Column (6) gives the bolometric amplitude, while the two subsequent columns report the amplitude of static (7) and effective (8) logarithmic surface gravity. The static gravity is referred to the surface zone, whereas the effective gravity has been evaluated by adopting the method suggested by Bono, Caputo & Stellingwerf (1994). Columns (9) and (10) give the amplitude of the surface temperature. The former is referred to the temperature of the outer boundary, whereas the latter is derived taking into account the surface variations over a full cycle of both luminosity and radius. The final column shows the pulsational amplitude in the V band (see §3 concerning the transformation into the observative plane).

In order to point out *who is doing what* concerning the driving and the damping of the pulsation instability, Figure 2 shows the total work curves referred to a fundamental model centrally located in the instability strip ($\log L/L_\odot = 3.07$,

$T_e=5800$ K). The light and velocity curves of this model are shown in Figure 1. Since we are interested in disclosing the destabilization effects of different elements (H, He, metals), the total work terms have been evaluated according to the relation $dW/d(\log \langle T \rangle)$, where $\langle T \rangle$ is the time average temperature per zone over a full cycle (see Bono et al. 1997a). Note that in the literature the total works are generally evaluated as a function of the exterior mass (i.e. $dW/d(\log M_e)$). According to Figure 2 we find that H and He, as expected, are the main destabilization sources whereas the Z-bump, at least for the assumed metallicity, barely affects the pulsation stability. On the other hand, the region located between the HeII ionization zone and the Z-bump is the main radiative damping region of the envelope. Moreover, the artificial viscosity pressure does not affect at all the physical structure of this model, since it is vanishing throughout the envelope. Turbulent and eddy viscosity pressure terms supply a non-negligible amount of dissipation in the hydrogen and helium ionization regions which in turn reduces the pulsational amplitudes.

In order to easily identify the opacity bumps which cause the appearance of both driving and damping regions, the bottom panel of Figure 2 shows the opacity excursions throughout the envelope structure. The opacity bump which appears in the outermost regions is worth mentioning. This opacity increment, at densities typical of Cepheid surface layers, is mainly due to H^- and partially to the Rayleigh scattering of hydrogen (see Fig. 7 in Alexander & Ferguson 1994). In fact, during a large part of the pulsation cycle the surface layers of this model oscillate at temperatures lower than 5,000 K, reaching the maximum temperature excursion ($T=5,250$ K) only around the phases of the luminosity maximum.

This feature, which has a negligible effect on the pulsation driving, could play a key role in the smoothness of both light and velocity curves. In fact, thanks to the inclusion of molecular opacities, the radial displacement of surface layers located above the hydrogen ionization region is governed by the physical excursion of temperature and density.

3 COMPARISON WITH OBSERVATIONS

In this section theoretical results are compared with the photometric data for NGC 1866 provided by WCFMM. These data refer to only nine out of the 23 Cepheids identified in NGC 1866, since photometry is not provided in the quoted paper for the remainder. In a subsequent paper Welch & Stetson (1993) applied their variable star detection technique to several frames centered on NGC 1866 and provided periods for all but one variable of the whole sample. However, both mean magnitudes and colours presented in that paper are affected by a poor photometric accuracy due to the crowding of central regions and thus are of no use.

Theoretical boundaries for both fundamental and first overtone instability strips ($Z=0.008$, $Y=0.25$ and $M = 5M_\odot$) have been transformed into the observative plane V-(B-V) by using Kurucz's bolometric corrections and colour-temperature relations (Kurucz 1992). In Figure 3 the transformed boundaries are shown together with the observed Cepheids of NGC 1866 studied by WCFMM. Following WCFMM discussion we have assumed for the cluster a reddening value $E(B-V)=0.06$ mag. and a distance modulus

Figure 2. *Top:* Full amplitude nonlinear total work curves versus the logarithmic time average temperature, surface at right. This fundamental model is centrally located in the instability strip ($\log L/L_\odot=3.07$; $T_e=5800$ K). The solid line shows the total work, the dashed line the turbulent work (i.e. the work due to both turbulent and eddy viscosity pressure), and the dashed-dotted line the artificial viscosity work. Positive and negative areas denote driving and damping regions respectively. *Bottom:* Logarithmic opacity of the envelope as a function of the logarithmic time average temperature. The opacity profile has been plotted at each time step over a full cycle. The arrows mark the location of the main opacity sources.

$DM=18.57$ mag. Solid lines represent, left to right, the First Overtone Blue Edge (FOBE), the Fundamental Blue Edge (FBE), the First Overtone Red Edge (FORE) and the Fundamental Red Edge (FRE). The FOBE and the FBE intersect at $\log L/L_\odot \approx 3.4$ and therefore we expect that above this luminosity level the instability strip is populated only by fundamental pulsators. Indeed at $\log L/L_\odot = 3.6$ the nonlinear models computed by adopting the linear first overtone radial eigenfunction do not show a stable limit cycle. On the other hand, toward lower luminosities, the FBE and the FORE intersect at $\log L/L_\odot = 2.8$, thus removing completely the "OR region", i.e. the region of the instability strip where pulsators are characterized by a stable limit cycle in the fundamental and in the first overtone mode.

The agreement with observational data appears satisfactory, since most of the observed variables are located well inside the theoretical instability strip around a magnitude level corresponding roughly to $\log L/L_\odot = 3.07$. In agreement with early results obtained by Bertelli et al. (1993), the comparison also suggests the occurrence of first overtone pulsators among Cepheids in NGC 1866. The only deviant variable is HV 12204, already pointed out by WCFMM for its peculiar brightness and blueness. However, from the analysis of radial velocities these authors concluded that HV 12204 is not a cluster member. Two further features of the instability strip are worth mentioning:

Figure 3. Fundamental and first overtone instability boundaries for $Z=0.008$, $Y=0.25$ and $M = 5M_{\odot}$. The observational data are referred to Cepheids in NGC 1866. See text for further details.

1) moving from higher to lower luminosities the instability strip becomes narrower; in the investigated luminosity range the colour width roughly decreases of a factor of two as the outer edges of the instability region present different slopes. These findings support the results obtained by Fernie (1990) for Galactic Cepheids and the preliminary trend suggested by Olszewski (1995) for Cepheids in LMC clusters.

2) The region of the instability strip in which only first overtones show a stable nonlinear limit cycle becomes larger at lower luminosities. This outcome supplies a straightforward but qualitative explanation for the large amount of first overtone pulsators -approximately 30 % of the total sample- recently detected by microlensing experiments (Beaulieu et al. 1995; Cook et al. 1995) and supports the hypothesis originally suggested by Böhm-Vitense (1988) concerning the occurrence of such variables among short-period Cepheids.

In Figure 4 the theoretical relations between periods and V amplitudes for both fundamental and first overtone models and for the labelled assumptions on luminosity are compared with the observational data provided by WCFMM. Bolometric amplitudes have been transformed into the V Johnson band by adopting Kurucz's static atmosphere models. The V magnitude curve can be used to derive either a magnitude-weighted amplitude or an intensity-weighted one, which is subsequently converted into magnitude units. The differences between amplitudes obtained from these two different approaches turned out to be negligible (less than 0.001 mag.).

It is worth noting that while the comparison in the HR diagram (instability strips) could be affected by uncertainties in the bolometric corrections, in the colour-temperature relations, in the reddening, and in the distance modulus, as well as in the method adopted to average the observed colours and magnitudes over the pulsation cycle, the comparison in the A_V - $\log P$ plane is independent of almost all these

Figure 4. Comparison in the Bailey diagram between predicted and observed V amplitudes and periods. Symbols are referred to different luminosity levels (see labelled values). Fundamental and first overtone amplitudes are plotted by adopting solid and dashed lines respectively. Asterisks show the observed V amplitudes provided by WCFMM.

troublesome effects, and is therefore far more robust. As a consequence, we can infer that Cepheids in NGC 1866, at least those for which photometric data are given in the literature (WCFMM), are well reproduced in the Bailey diagram by a sequence of pulsational models with $Z=0.008$, $Y=0.25$, $M = 5M_{\odot}$ and $\log L/L_{\odot} \simeq 3.07$, in remarkable agreement with the adopted evolutionary predictions. Note that the sequences of models characterized by the same values of stellar mass and chemical composition but by luminosity levels different from $\log L/L_{\odot} = 3.07$ are clearly unable to match observational data. This means that, in principle, the comparison in the period-amplitude diagram proves to be a powerful instrument for estimating the luminosity level of cluster Cepheids.

A further interesting aspect worth being investigated in order to provide both a suitable test of the present theoretical scenario and a tight constraint on the pulsation characteristics of classical Cepheids is the comparison between the Fourier parameters of theoretical and observed light curves (Simon & Kanbur 1995). Even though such analysis is clearly beyond the scope of this paper, a comprehensive comparison with observational data and the impact of the pulsation/convection interaction on observables will be discussed in a forthcoming paper (Bono & Marconi 1997).

4 CONCLUSIONS

The agreement between Cepheid theoretical models and the photometric data available in the literature provides a sound support to the plausibility of the physical assumptions adopted in the development of this new pulsational scenario. In a homogeneous theoretical context we derived both the blue and the red edges of the instability strip. In

particular, it is worth noting that the red edges have been evaluated without invoking any *ad hoc* assumption on the efficiency of the convective transport over the pulsation cycle. At the same time present limiting amplitude calculations strongly support the existence of first overtone pulsators among Cepheids. In fact, we found that there is a well defined region of the instability strip in which only first overtone pulsators present a nonlinear limit cycle stability. On the other hand, taking into account the distribution of pulsational amplitudes in the Bailey diagram we find that the luminosity level of Cepheids along the blue loop is in agreement with the value predicted by canonical evolutionary models.

However, a deeper insight on the matter is prevented by the limited sample of Cepheids currently available. What is relatively surprising about photometric data of young LMC clusters (see Table 2 in Welch, Mateo & Olszewski 1993 and references therein) with a good Cepheid sample is that even though they are the keystone for determining the P-L and the P-L-C relations on which rely the distance evaluations of the Local Group Galaxies, and in turn the calibration of secondary distance indicators, we still lack a comprehensive observational scenario for these objects.

Moreover, although several approaches have been recently undertaken for evaluating the metal abundance of stellar clusters in Magellanic Clouds (Geisler & Mateo 1989; Olszewski et al. 1991), a detailed analysis of the chemical composition spread of Cepheids in Galactic and Magellanic Clouds clusters is even more urgent.

As far as future theoretical developments are concerned, we plan to extend the present nonlinear pulsational scenario by taking into account different stellar masses and chemical compositions for properly disclosing the dependence of Cepheids behaviour on these astrophysical parameters.

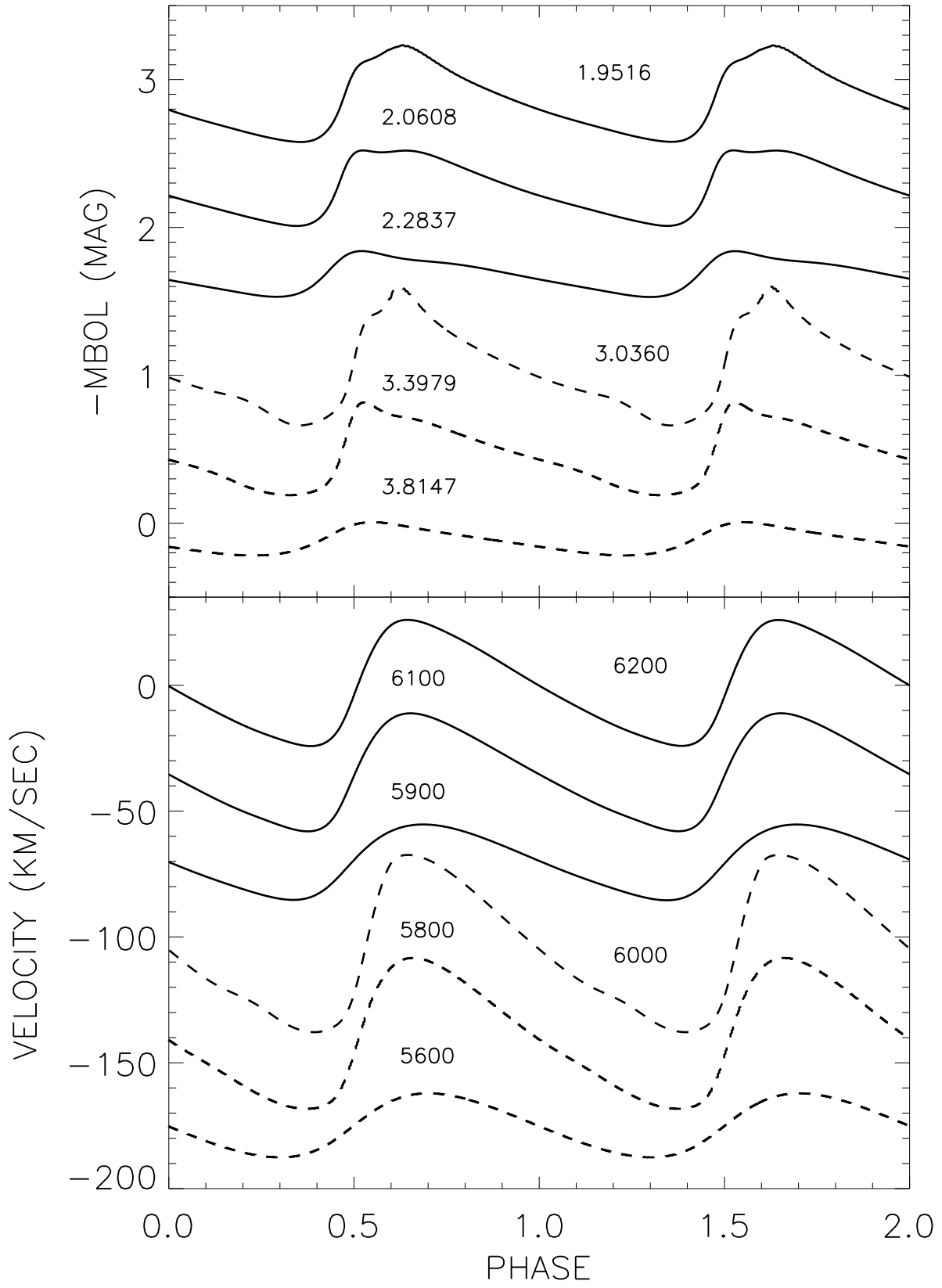
ACKNOWLEDGMENTS

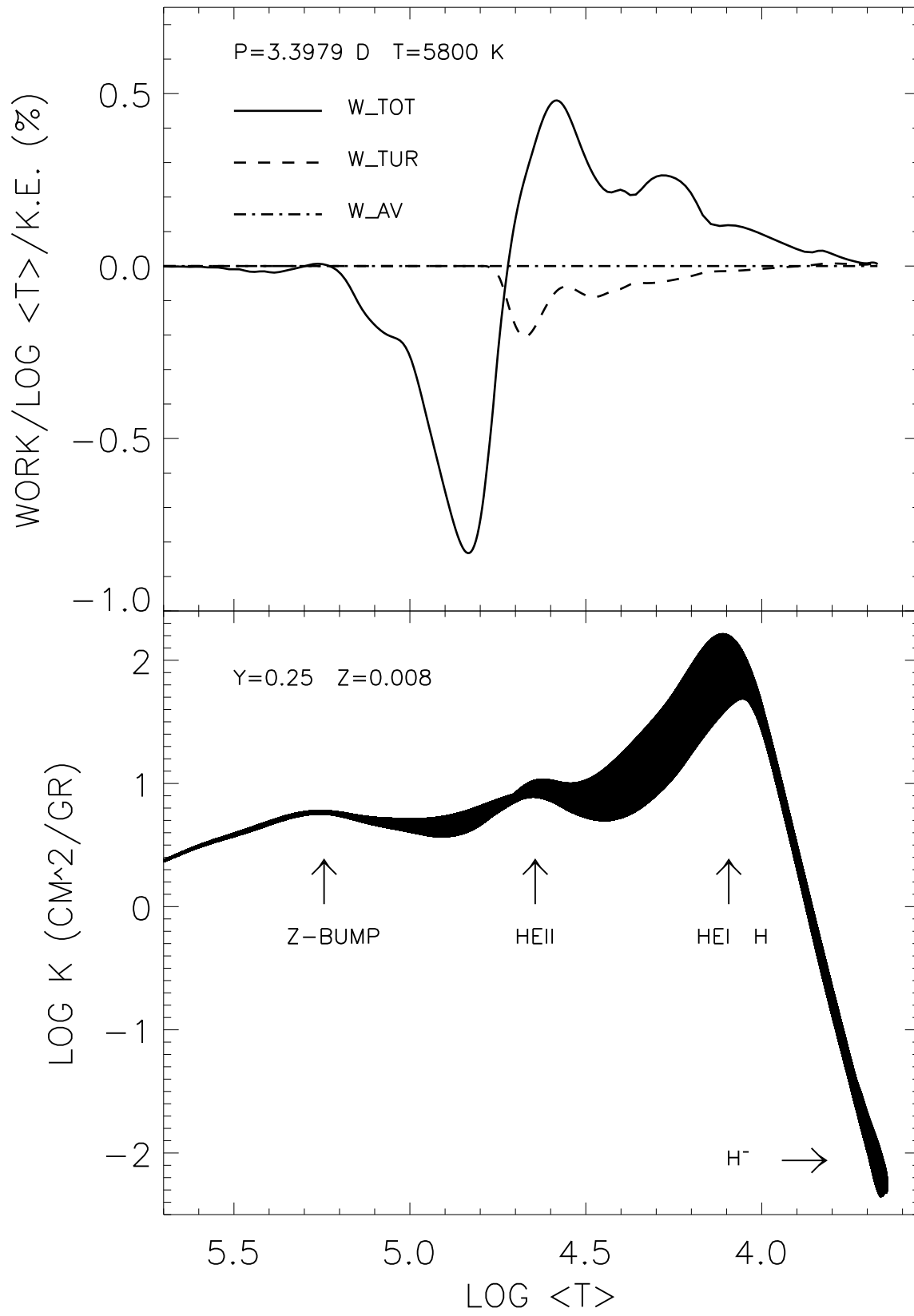
It is a pleasure to thank V. Castellani and F. Caputo for many warm and enlightening discussions on Cepheids and intermediate-mass stars.

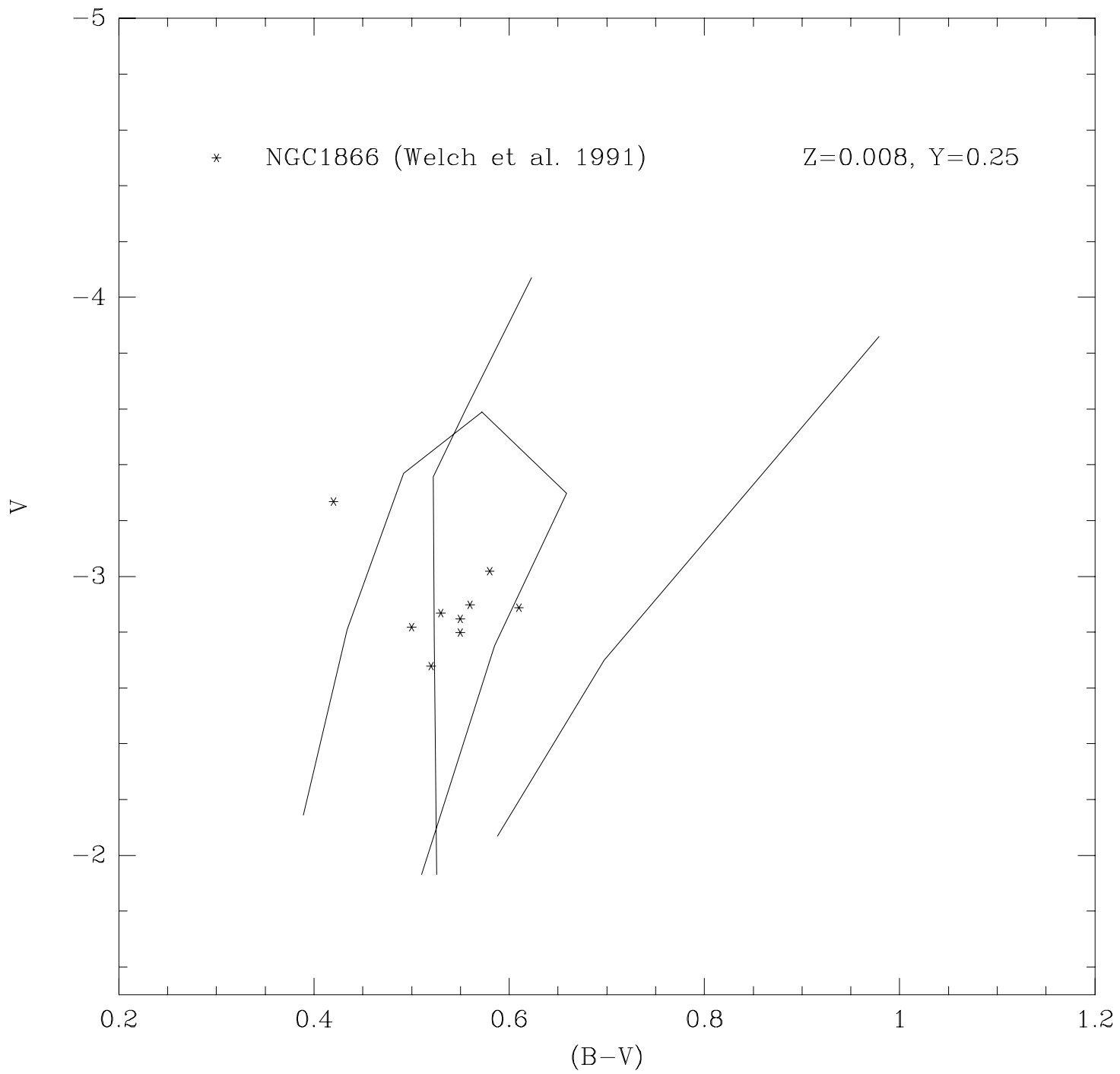
REFERENCES

- Alexander, D. R., & Ferguson, J. W. 1994, ApJ, 437, 879
 Arp, H. C. 1967, ApJ, 149, 91
 Beaulieu, J. P., et al. 1995, A&A, 303, 137
 Bertelli, G., Bressan, A., Chiosi, C., Mateo, M., & Wood, P. R. 1993, ApJ, 412, 160
 Böhm-Vitense, E. 1988, ApJ, 324, L27
 Bono, G., Caputo, F., Cassisi, S., Castellani, V., & Marconi, M. 1997a, ApJ, submitted
 Bono, G., Caputo, F., Castellani, V., & Marconi, M. 1997b, A&AS, 121, 327
 Bono, G., Caputo, F., & Stellingwerf, R. F. 1994, ApJ, L51
 Bono, G., Incerpi, R., & Marconi, M. 1996, ApJ, 467, L97
 Bono, G., & Marconi, M. 1997, in preparation
 Bono, G., & Stellingwerf, R. F. 1993, Mem. Soc. Astron. It., 64, 559
 Bono, G., & Stellingwerf, R. F. 1994, ApJS, 93, 233
 Brocato, E., Castellani, V., & Piersimoni, A. M. 1994, A&A, 290, 59
 Buchler, J. R., Kollath, Z., Beaulieu, J. P., & Goupil, M. J. 1996, ApJ, 462, 83L
 Carson, T. R., & Stothers, R. B. 1984, ApJ, 276, 593
 Chiosi, C., Bertelli, G., Meylan, G., & Ortolani, S. 1989, A&A, 219, 167
 Chiosi, C., Wood, P., Bertelli, G., & Bressan, A. 1992, ApJ, 387, 320
 Chiosi, C., Wood, P. R., & Capitanio, N. 1993, ApJS, 86, 541
 Cook, K. H., et al. 1995, in IAU Colloq. 155, Astrophysical Applications of Stellar Pulsation, eds. R.S. Stobie & P.A. Whitelock (San Francisco: ASP), 83, 221
 Dufour, R. J. 1984, in IAU Symp. 108, Structure and Evolution of the Magellanic Clouds, ed. S. van den Bergh & K.S. de Boer (Dordrecht: Reidel), 353
 Fernie, J. D. 1990, ApJ, 354, 295
 Geisler, D., & Mateo, M. 1989, RMxAA, 19, 101
 Iglesias, C. A., & Rogers, F. J. 1996, ApJ, 464, 943
 Karp, A. H. 1975, ApJ, 201, 641
 Kurucz, R. L. 1992, in IAU Symp. 149, The Stellar Populations of Galaxies, eds. B. Barbury & A. Renzini (Dordrecht: Kluwer), 225
 Morgan, S. M., & Welch, D. L. 1996, preprint, astro-ph/9607068
 Olszewski, E. W. 1995, in IAU Symp. 164, Stellar Populations, eds. P.C. van der Kruit & G. Gilmore (Dordrecht: Kluwer), 181
 Olszewski, E. W., Schommer, R. A., Suntzeff, N. B., & Harris, H. C. 1991, AJ, 101, 515
 Russell, S. C., & Bessel, M. S. 1989, ApJS, 70, 865
 Russell, S. C., & Dopita, M. A. 1990, ApJS, 74, 93
 Sebo, K. M., & Wood, P. R. 1995, ApJ, 449, 164
 Simon, N. R., & Kanbur, S. M. 1995, ApJ, 451, 703
 Walker, M. F. 1974, MNRAS, 169, 199
 Walker, A. R. 1987, MNRAS, 225, 627
 Welch, D. L., Cote, P., Fisher, P., Mateo, M., & Madore, B. F. 1991, AJ, 101, 490 (WCFMM)
 Welch, D. L., Mateo, M., & Olszewski, E. W. 1993, in IAU Colloq. 139, New Perspectives on Stellar Pulsation and Pulsating Variable Stars, eds. J.M. Nemeč & J.M. Matthews (Cambridge: Cambridge Univ. Press), 359
 Welch, D. L., & Stetson, P. B. 1993, AJ, 105, 1813

This paper has been produced using the Blackwell Scientific Publications \TeX macros.







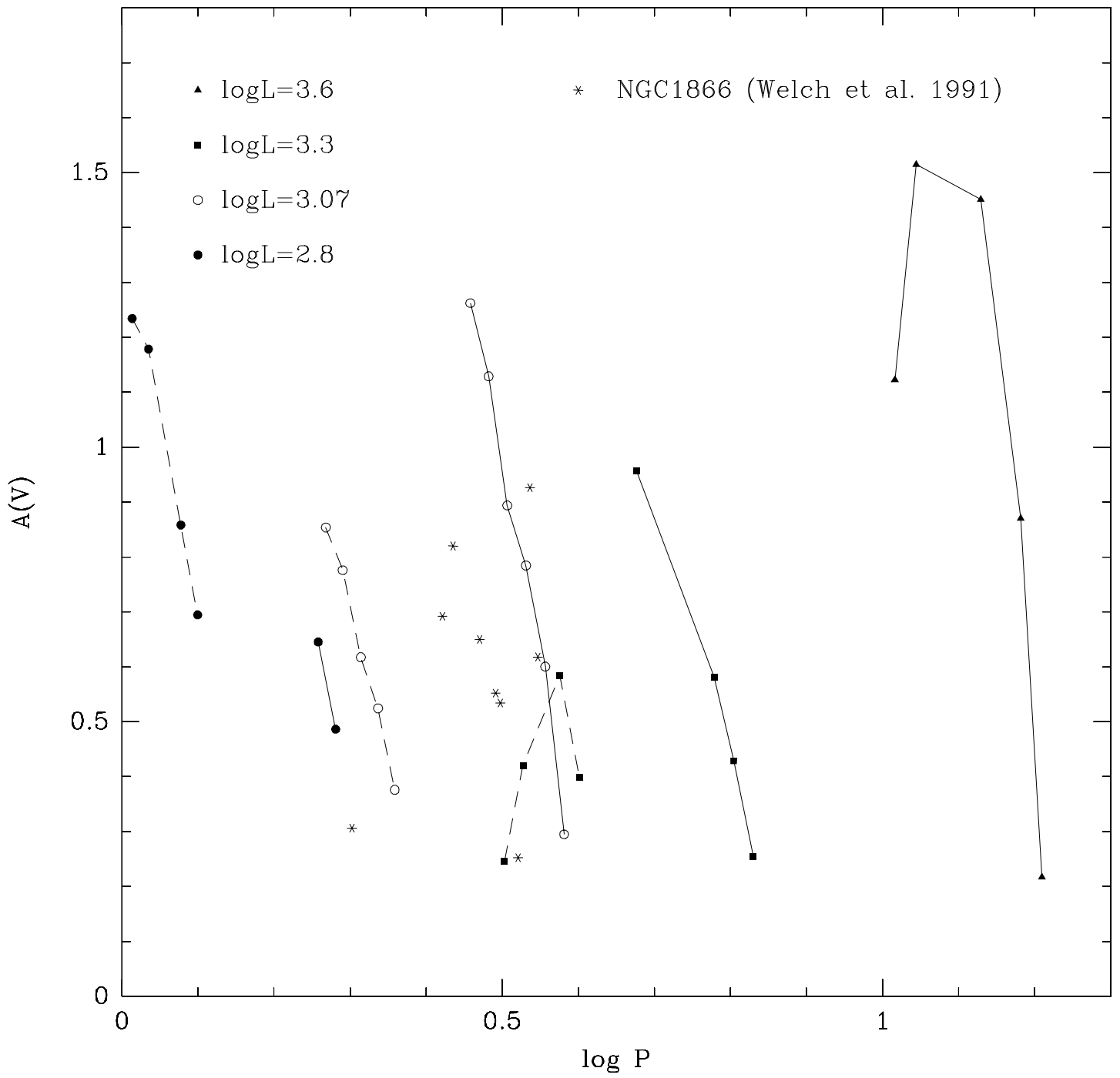


TABLE 1
NONLINEAR SURVEY: OBSERVABLES

$\log L/L_{\odot}$ ^a	T_e ^b	P ^c	$\Delta R/R_{ph}$ ^d	Δu ^e	ΔM_{bol} ^f	$\Delta \log g_s$ ^g	$\Delta \log g_{eff}$ ^h	ΔT ⁱ	ΔT_e ^j	A_V ^k
First Overtone										
2.80	6500	1.0318	0.072	70.93	1.109	0.06	0.74	1500	1850	1.234
2.80	6400	1.0842	0.110	78.15	1.033	0.07	0.81	1400	1700	1.179
2.80	6200	1.1952	0.078	72.03	0.714	0.07	0.81	1000	1200	0.858
2.80	6100	1.2575	0.067	58.08	0.570	0.06	0.68	800	1000	0.695
3.07	6300	1.8539	0.058	46.53	0.733	0.05	0.59	900	1150	0.854
3.07	6200	1.9516	0.062	50.06	0.654	0.05	0.62	800	1000	0.776
3.07	6100	2.0608	0.059	46.88	0.511	0.05	0.58	650	800	0.617
3.07	6000	2.1710	0.052	40.18	0.433	0.05	0.49	550	700	0.524
3.07	5900	2.2837	0.040	29.87	0.307	0.03	0.37	400	500	0.376
3.30	6100	3.1841	0.022	13.78	0.205	0.02	0.18	250	300	0.246
3.30	6000	3.3673	0.040	24.50	0.345	0.03	0.34	400	500	0.420
3.30	5800	3.7647	0.066	41.24	0.469	0.06	0.52	600	700	0.584
3.30	5700	3.9931	0.050	29.79	0.313	0.04	0.39	400	500	0.398
Fundamental										
2.80	6000	1.8119	0.095	63.09	0.520	0.08	0.55	750	950	0.645
2.80	5900	1.9100	0.076	48.79	0.396	0.07	0.42	600	700	0.487
3.07	6100	2.8722	0.119	65.74	1.078	0.10	0.69	1350	1700	1.262
3.07	6000	3.0360	0.128	70.40	0.938	0.11	0.74	1150	1450	1.129
3.07	5900	3.2112	0.126	68.11	0.725	0.11	0.73	950	1200	0.894
3.07	5800	3.3979	0.115	59.99	0.624	0.10	0.63	850	1050	0.785
3.07	5700	3.6030	0.095	47.62	0.478	0.08	0.49	650	800	0.600
3.07	5600	3.8147	0.053	25.43	0.225	0.04	0.25	300	400	0.295
3.30	6000	4.7509	0.084	37.53	0.712	0.08	0.47	950	1200	0.956
3.30	5600	6.0050	0.086	38.09	0.444	0.08	0.42	550	700	0.582
3.30	5500	6.3743	0.068	29.98	0.317	0.06	0.32	400	500	0.429
3.30	5400	6.7647	0.043	17.54	0.183	0.04	0.19	250	300	0.254
3.60	5700	10.3780	0.129	45.57	0.877	0.11	0.56	1100	1350	1.123
3.60	5600	11.0760	0.176	61.51	1.186	0.15	0.86	1500	1850	1.515
3.60	5300	13.4600	0.212	66.52	1.033	0.18	0.90	1300	1600	1.451
3.60	5100	15.1911	0.146	40.11	0.585	0.13	0.57	800	950	0.870
3.60	5000	16.2010	0.046	11.98	0.136	0.04	0.16	200	250	0.217

^a Logarithmic luminosity (solar units). ^b Effective temperature (K). ^c Period (days). ^d Fractional radius variation.
^e Radial velocity amplitude (Km/s). ^f Bolometric amplitude (mag.). ^g Amplitude of logarithmic static gravity.
^h Amplitude of logarithmic effective gravity. ⁱ Surface temperature variation. ^j Effective temperature variation.
^k Visual amplitude (mag.).